



HAL
open science

Fracture Properties of Kerogen and Importance for Organic-Rich Shales

Laurent Brochard, György Hantal, Hadrien Laubie, R.J.M. Pellenq, Franz-Joseph
Ulm

► **To cite this version:**

Laurent Brochard, György Hantal, Hadrien Laubie, R.J.M. Pellenq, Franz-Joseph Ulm. Fracture Properties of Kerogen and Importance for Organic-Rich Shales. Annual world conference on Carbon (Carbon 2013), Jul 2013, Rio de Janeiro, Brazil. <hal-01274161>

HAL Id: hal-01274161

<https://hal.science/hal-01274161v1>

Submitted on 15 Feb 2016

HAL is a multi-disciplinary open access archive for the deposit and dissemination of scientific research documents, whether they are published or not. The documents may come from teaching and research institutions in France or abroad, or from public or private research centers.

L'archive ouverte pluridisciplinaire **HAL**, est destinée au dépôt et à la diffusion de documents scientifiques de niveau recherche, publiés ou non, émanant des établissements d'enseignement et de recherche français ou étrangers, des laboratoires publics ou privés.



HAL Authorization

FRACTURE PROPERTIES OF KEROGEN AND IMPORTANCE FOR ORGANIC-RICH SHALES

Laurent Brochard^{a*}, György Hantal^b, Hadrien Laubie^b,
Roland J.-M. Pellenq^{b,c} and Franz J. Ulm^b

^a Université Paris-Est, Laboratoire Navier (UMR 8205), CNRS/ENPC/IFSTTAR, 77455 Marne-la-Vallée, France.

^b MIT, Civil and Environmental Engineering, 77 Massachusetts Avenue, 02139, Cambridge, MA, USA.

^c CINA-M-CNRS, Campus de Luminy, 13288 Marseille cedex 09, France.

*laurent.brochard@enpc.fr

Introduction

Oil and gas produced from organic-rich shales have become in the last ten years one of the most promising sources of unconventional fossil fuels. The oil and gas are trapped in rocks of very small permeability, but hydraulic fracturing enables to operate those reservoirs with competitive costs. The global reserves of shale oil and gas that are potentially recoverable are equivalent to tens of years of world consumption. However, hydraulic fracturing is facing many challenges regarding the productivity but also the security and the environment. One of those challenges is to understand how the fractures propagate underground. The propagation depends on the mechanical stress prevailing in the reservoir and on the fracture properties of the rocks. Regarding the fracture properties, the oil and gas industry developed brittleness indicators to distinguish between brittle rocks (containing mostly calcite and silica) and ductile rocks (containing a significant proportion of clay and kerogen). During fracturing, a brittle rock shatters easily leading to a well-distributed network of fractures, whereas a ductile rock deforms instead of shattering leading to few fractures and in some situations acting as a barrier to the fracture propagation. In this work, we study the role of kerogen in the ductility of shale. The ultimate objective is to develop a fine understanding of the fracture properties of shales.

Methodology

Organic-rich shales are heterogeneous materials containing a small fraction of kerogen. The typical size of the kerogen heterogeneities is a micrometer or less, and, therefore, mechanical tests on these materials are usually performed at the scale of the heterogeneous medium. Measuring the fracture properties of kerogen and of its interface with minerals is very challenging. As an alternative to laboratory experiments, we use molecular simulations to estimate fracture properties at the nanometer scale. As a preliminary work, we develop a methodology to estimate fracture properties and validate it against experimental data in the

case of silica, a common mineral in shale reservoirs and a good benchmark in our work.

By simulating fracture propagation by molecular simulations one can estimate the fracture properties of a material. At the atomic scale, crack propagation results of complex atomic rearrangements at the crack tip whereas, at the macroscopic scale, one refers to the simplified notions of toughness and ductility. In this work, we propose an approach by thermodynamic integration to capture the toughness and ductility from the results of a molecular simulation. This approach relies on the energetic theory of fracture mechanics [1].

We consider a molecular system in which we initiate a crack and we load the system to propagate this initial crack. Assuming isothermal condition, this loading leads to an increase of free energy F of the system which can be converted either into mechanical energy P by deforming the solid or into fracture energy G_c by propagating the crack. The energy balance of the system is

$$dF = dP + G_c dA \quad (1)$$

The quantity G_c , also known as critical energy release rate, characterizes the fracture properties of the material: G_c is related to the fracture toughness K_{Ic} through Irwin's formula [1] and its extension to anisotropic materials [2]. For a perfectly brittle material, $G_c = 2\gamma$ where γ is the surface energy of the material; but for ductile materials G_c is much larger than 2γ because of significant irreversibility at the crack tip during the crack propagation, e.g., plasticity. Therefore, G_c is also an indicator of the level of ductility of the material.

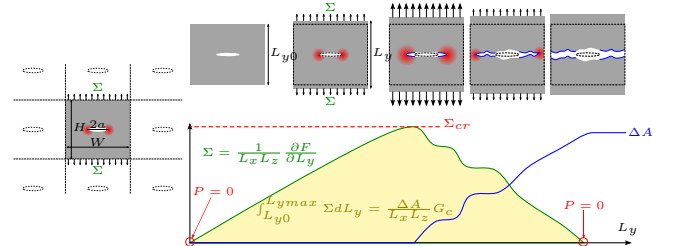


Fig. 1 Schematic description of the geometry of the molecular systems and of the procedure of thermodynamic integration.

We consider systems whose general geometry is displayed in Figure 1: the system is periodic with an elliptic hole at the center of the system which corresponds to a through-crack. We also display in Figure 1 a schematic description of the procedure we follow for the thermodynamic integration. The derivative of the free energy $\Sigma = \frac{1}{L_x L_z} \frac{\partial F}{\partial L_y} \Big|_{T, L_x, L_z}$ can be interpreted as the average stress along the top and bottom boundaries of system. The main steps of the procedure are the following: 1 - At the beginning of the simulation, the system is relaxed mechanically and, accordingly, $P = 0$. 2 - We load the system by

increasing the length L_y in the direction orthogonal to the crack. 3 - At the beginning, the loading is too small to propagate the crack and all the free energy is stored in the form of mechanical energy. 4 - When the loading is large enough, some irreversible processes may occur at the crack tip and the crack starts to propagate. At that point, Σ reaches its maximum and mechanical energy starts to be converted into fracture energy. 5 - At the end of the procedure, the crack fully propagated over the whole system. As at the beginning of the procedure, $P = 0$.

The thermodynamic integration consists in integrating Σ over the whole loading procedure. Since $P = 0$ both at the beginning and at the end of the procedure, all the variation of free energy (Eq. 1) corresponds to fracture energy only:

$$G_c = \frac{\Delta F}{\Delta A} = \frac{L_x L_z}{\Delta A} \int_{L_{y0}}^{L_{ymax}} \Sigma dL_y \quad (2)$$

Therefore, with this methodology, we can estimate the fracture properties, i.e., toughness and ductility, starting from the elementary inter-atomic interactions. The detailed description of the methodology and its main limitations are presented in [3].

The relevance of this estimation relies on the reliability of the inter-atomic potential we consider. In particular, to properly simulate fracture processes, this energy potential must be able to predict complex atomic rearrangements such as bond breaking / formation or transfer of charges. In this work, we consider the reactive potential reaxFF [4] parameterized for system made of Si-O-C-H [5]. We benchmarked the applicability of this potential to silica-kerogen system by comparing the energy computed with reaxFF and that computed with ab-initio methods for a series of elementary chemical bonds that are present in those systems [6].

Validation

Before applying this methodology to kerogen, we validate it against experimental data and against the usual theory of Linear Elastic Fracture Mechanics (LEFM). Silica, which is a common mineral in shale reservoirs, is a good benchmark for the methodology we proposed: experimental data are available, and LEFM applies well to this material even at small scale since it is a homogeneous brittle material.

We consider α -cristobalite, a silica crystal metastable in ambient conditions. This particular silica is convenient regarding the forthcoming study of the kerogen-silica interface, because its crystalline structure is orthorhombic and its size adapts very well to the lattice of the kerogen molecular reconstruction we consider later on. We investigate a total of 33 different systems varying the size of the initial crack, the size of the whole system, the orientation of the crack. The detail of the systems studied and the numerical aspects of the simulations are available in [3]. In this work, we present the results of 18 of those systems (long procedure in [3]).

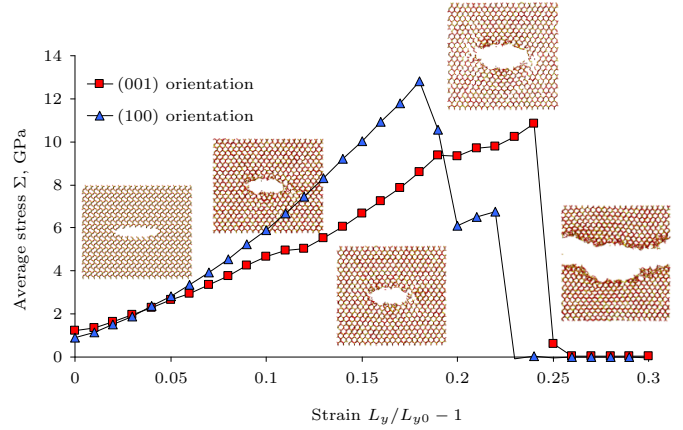


Fig. 2 Strain-stress curves for two of the α -cristobalite systems studied.

We display in Figure 2 the evolution of Σ during the loading procedure for two of the systems studied, one with the crack in the (001) orientation, and the other with the crack in the (100) orientation. In addition we illustrate the strain-stress curve with a few snapshots of molecular configurations for the first system (001) orientation. The crack propagation in α -cristobalite is very sudden, characteristic of a brittle behavior, although we observe some arrest in the propagation as is the case for the second system in Figure 2.

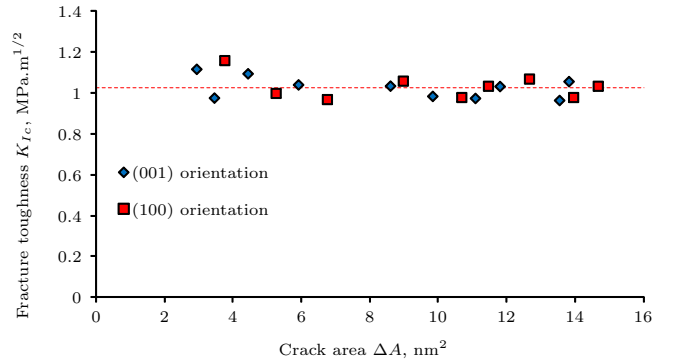


Fig. 3 Fracture toughness of α -cristobalite estimated by thermodynamic integration.

Since the different systems studied have different geometries, the strain and the stress at the onset of propagation always differ from one system to another. However, the thermodynamic integration should provide a similar energy release rate G_c for all the systems. We display in Figure 3 the fracture toughness estimated in function of the area of crack created ΔA . The fracture toughness K_{Ic} is derived from the critical energy release rate G_c with the extension of Irwin's formula to orthotropic materials [2]. The values of all those systems are very consistent and independent of the geometry. Based on thermodynamic

integration, the average toughness is $1.03 \text{ MPa}\cdot\text{m}^{1/2}$. This result compares well with the value generally measured experimentally for silica [7]: $0.82 \pm 0.07 \text{ MPa}\cdot\text{m}^{1/2}$.

In addition, we can validate the methodology against LEFM. Silica is a linear elastic brittle material and therefore LEFM should be valid in the case of silica. According to LEFM, the critical stress Σ_{cr} at the onset of crack propagation is related to the toughness K_{Ic} according to:

$$\frac{K_{Ic}}{\Sigma_{cr}\sqrt{\pi a}} = C \quad (3)$$

where C is a coefficient that depends on the geometry of the system. In the case of the periodic system we consider here (see Figure 1), C depends only on the ratios a/W and H/W and can be computed numerically [8]. We represent in Figure 4 the critical stress in function of the effective crack length $\pi a_{eff} = \pi a C^2$ for the various systems of α -cristobalite simulated. The relationship between the critical stress and the effective length is consistent with Eq. 3. From Eq. 3, we estimate toughnesses of 0.87 and $0.81 \text{ MPa}\cdot\text{m}^{1/2}$ for the crack orientations (001) and (100), respectively. These results compare well with that obtain from thermodynamic integration and with the experimental results. Accordingly, the approach we propose applies well in the case of α -cristobalite.

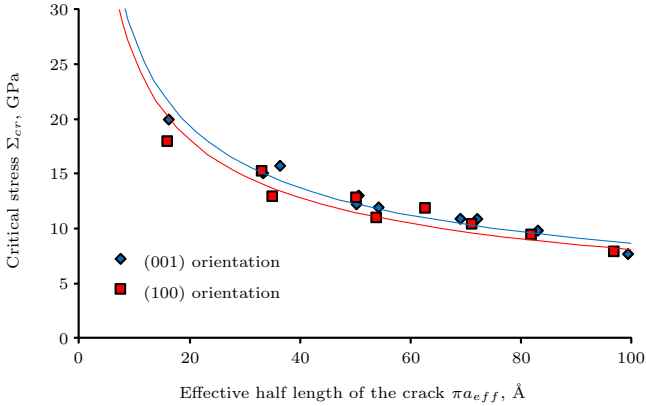


Fig. 4 Critical stress in function of the crack length and fit with Eq. 3 (LEFM) for α -cristobalite.

Fracture properties of kerogen

Kerogen is a generic word that encompasses all the solid organic matter that is present in shale reservoir. There is not a unique molecular structure of kerogen but a large variety of possible structures. In this work, we study a molecular structure of microporous carbon, CS1000 [9], that is similar to dense mature kerogen, i.e., dense kerogen with low hydrogen and oxygen contents. Accordingly, the results of this section cannot be considered as representative of all types of kerogen. Nevertheless, the most interesting reservoirs in terms of shale gas recovery are those filled with mature kerogen, for which CS1000 is a reasonable molecular representation.

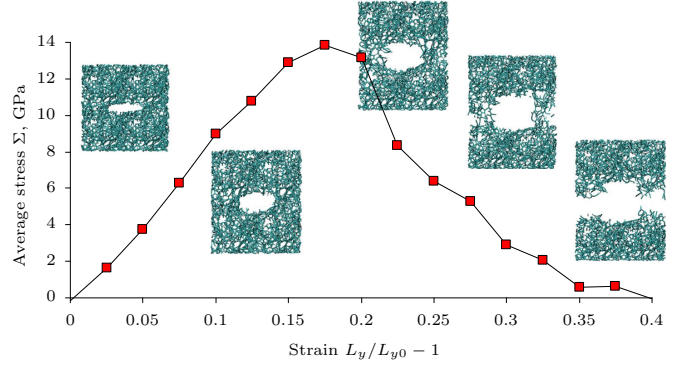


Fig. 5 Strain-stress curve for one of the CS1000 systems studied.

We consider a series of 25 systems for CS1000 varying the size of the crack and of the whole system and the positions of the crack in the heterogeneous structure. An example of strain-stress curve is displayed in Figure 5. As is readily visible, the crack propagation is not sudden like in the case of α -cristobalite: the material exhibits a significant ductility because of large rearrangements in the atomic structure at the crack tips. These rearrangements are irreversible processes that dissipate energy. Accordingly, we expect the fracture energy of CS1000 to be much larger than the surface energy. We computed the fracture energy (Eq. 2) and we display the results in function of the area of crack created in Figure 6. The results show a correlation with the area, that we interpret as a size effect: the overlap between the process zones at the periodic boundaries cannot be neglected. We propose a correction of the results to account for this overlap by reducing the actual area of crack created with a simplistic model (see [3]). The corrected results are displayed in Figure 6 and exhibit no more trend.

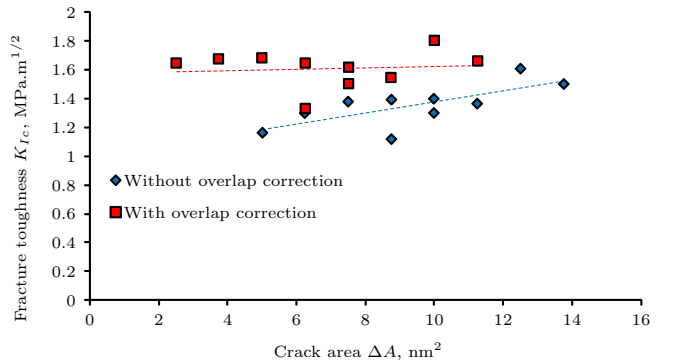


Fig. 6 Fracture toughness of CS1000 estimated by thermodynamic integration.

By thermodynamic integration, we estimate a toughness of $1.61 \text{ MPa}\cdot\text{m}^{1/2}$ for CS1000 which is about two times the value for α -cristobalite. As for α -cristobalite, we also

use LEFM to provide an alternative estimate of the toughness. We display in Figure 7 the critical stress in function of the effective crack length. It appears that the trend is not as consistent with Eq. 3 as in the case of α -cristobalite. The best fit with Eq. 3 leads to a toughness of $0.80 \text{ MPa}\cdot\text{m}^{1/2}$ two times smaller than the estimate from thermodynamic integration. This discrepancy stems to the fact that LEFM is not valid in the case of CS1000 at this scale because the size of the process zone cannot be neglected as was the case for silica. In contrast, the thermodynamic integration does not assume any material behavior and is valid even if the process zone is significant. The value of $1.61 \text{ MPa}\cdot\text{m}^{1/2}$ can be considered as a good estimation of the actual toughness of CS1000.

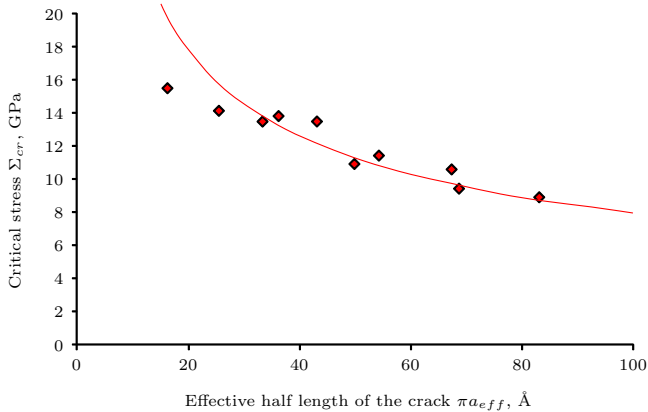


Fig. 7 Critical stress in function of the crack length and fit with Eq. 3 (LEFM) for CS1000.

This toughness corresponds to an energy release rate G_c about 12 times larger than the surface energy of CS1000, that is a very significant ductility. The ductility is readily visible in Figure 5 (strain-stress curve): the ratio between the maximum strain (0.4) and the maximum stress at failure (14 GPa) is two times larger than in the case of α -cristobalite for similar geometries. These results are consistent with the ductility observed at the scale of shale rocks (increase of ductility with kerogen content). However, the absolute value of toughness obtained for CS1000 should not be considered as representative of all mature kerogen since it is very dependent on the density; and the density of CS1000 ($1.6 \text{ kg}\cdot\text{m}^{-3}$) corresponds to the density of the microporous part of kerogen, i.e., kerogen excluding meso- and macro-pores. Accordingly the toughness of CS1000 is in the upper range of values for mature kerogen.

Fracture at the kerogen-silica interface

At the scale of the heterogeneous material, the effective fracture properties may strongly depend on the properties of the interface and not only on the properties of the elementary phases. If cracking at the scale of the heterogeneous shale never occurs in the kerogen phase, but only

at the kerogen / mineral interface, the ductility of kerogen itself is not enough to explain the ductility of the shale. For this reason, this section is dedicated to the CS1000 / α -cristobalite interface.

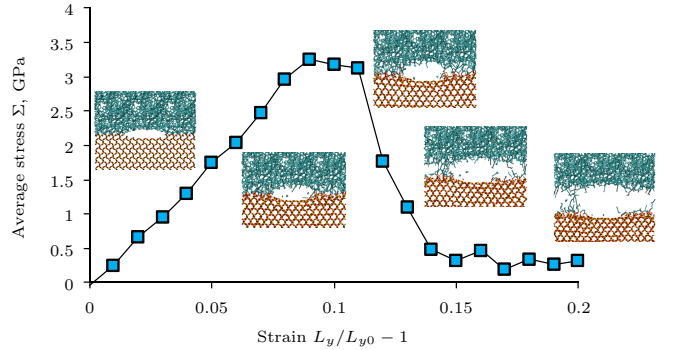


Fig. 8 Strain-stress curve for one of the α -cristobalite / CS1000 interfaces studied.

In a separate work, we reconstructed a series of 11 typical interfaces by studying the bonding at the interface between kerogen and silica by quantum calculations [6]. We then applied the same methodology to these interfaces as we did for CS1000 and α -cristobalite, with an initial crack initiated along the interface. In Figure 8, we display the strain-stress curve for one of the system simulated. The interface exhibits some ductility as CS1000, but mostly on the side of CS1000 and not in α -cristobalite. The crack propagation is not sudden and the shape of the strain-stress curve looks similar to that of CS1000 (Figure 5). However, the value of the critical stress is much smaller than for the bulk materials. As a consequence, the thermodynamic integration leads to an average toughness of $0.57 \text{ MPa}\cdot\text{m}^{1/2}$, smaller than for the bulk materials. Now, this toughness value is not small when considering the number of covalent bonds at the interface: only 37% of the Si-O terminations of the α -cristobalite surface are bonded to the kerogen.

Even though the absolute toughness is small, the interface is still ductile. Indeed, applying the LEFM Eq. 3, we obtain a value of toughness for the interface of $0.26 \text{ MPa}\cdot\text{m}^{1/2}$, more than two times smaller than the value obtain by thermodynamic integration. Therefore, the ductility of the interface looks very similar to the ductility of bulk CS1000, which supports the experimental observations at the scale of shale rocks.

From kerogen to heterogeneous shale rocks

In the previous section, we focused on two elementary constituents of shales rocks and their interface, and we found that kerogen and kerogen-silica interface are quite ductile. However, what matters for field applications is the ductility of the shale rock which depends not only on the fracture properties of the elementary constituents and their interface, but also on the microstructure. As an illustra-

tion of the potential increase of ductility due to the presence of kerogen, we consider here the case of a particular geometry in which the kerogen is located in spherical pockets distributed periodically in a homogeneous mineral matrix (Figure 9). In such geometry, the ductile pockets may form bridges in the wake of a propagating crack [10]. Since the fracture energy of the interface is 14% of the fracture energy of bulk kerogen, the bridges eventually debond at their interface with the brittle matrix [11]. This phenomenon, called particle pull out, is known to significantly increase the resistance to fracture propagation.

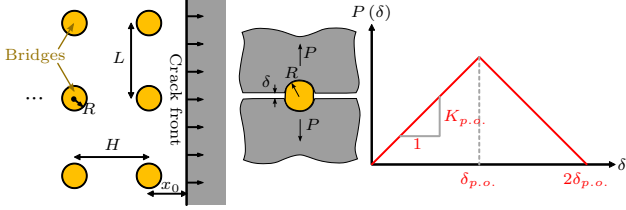


Fig. 9 Model considered for the particle pull out phenomenon.

In this work, we use the numerical approach of Bower et al. [10] to compute numerically the increase of the effective toughness K_{Ic}^{eff} due to the particle pull out phenomenon. Each pocket of kerogen exerts a bridging force P on the crack faces that depend on the crack opening δ . Following the numerical approach of Bower et al., the relative increase in toughness $K_{Ic}^{eff}/K_{Ic}^{matrix}$ depends on the pull out law $P = P(\delta)$, and on the geometry of the system ($R/L, H/L, x_0/L$). In our work, we considered the pull out law displayed in Figure 9 which is inspired from the shape of the strain-stress curve obtained by molecular simulation of crack propagation at the interface (Figure 8). The values of the parameters $K_{p.o.}$ and $\delta_{p.o.}$ are related to the energy release rate at the interface. Assuming spherical particles debonded on half of their interface with the matrix, we have: $2\pi R^2 G_c^{interface} = \int_0^{2\delta_{p.o.}} P(\delta) d\delta = K_{p.o.} (\delta_{p.o.})^2$. In what follows, we varied $K_{p.o.}$ and $\delta_{p.o.}$ while ensuring this condition on energy release. As a starting value, we considered a high value of the elasticity of the particle pull-out equal to the elasticity of the matrix: $K_{p.o.}^{ref} = (2\pi RE)/(2(1-\nu^2))$, where E and ν are the Young's modulus and Poisson's ratio of the matrix.

In Figure 10, we display the relative increase in toughness in function of the surface fraction of ductile particle for various pull out elasticity $K_{p.o.}$. The increase in toughness is important, up to a factor of 3 for as little as 20% of ductile particles. In the specific case of kerogen and silica, $K_{Ic}^{interface}/K_{Ic}^{matrix} = 0.7$ from the molecular simulations, and the elasticity of kerogen is usually estimated around 10 GPa, i.e. $K_{p.o.}/K_{p.o.}^{ref} \approx 0.125$. In those conditions, the relative increase of toughness is 2 for a fraction of kerogen of 10% and 3 for a fraction of kerogen of 20%.

Of course not all kerogen in shale does form bridges

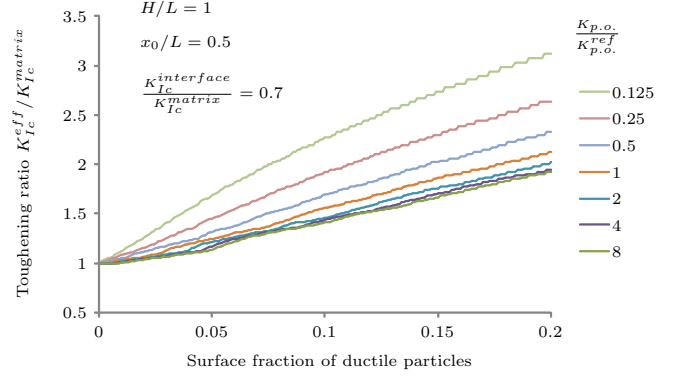


Fig. 10 Relative increase in toughness.

and the geometry considered is very simplistic. But this calculation shows that even a small fraction of ductile particle can significantly affect the fracture properties of the shale rock. Kerogen is not the only ductile material in shale: clays also increase the ductility of shale. Therefore a general picture of the ductility of shale requires accounting for the presence of clay and not only of kerogen.

Conclusion

We performed molecular simulations to study the fracture properties of kerogen, silica and their interface. First, we developed a specific methodology based on a thermodynamic integration to estimate the fracture properties by molecular simulation and we validated this approach against experimental data and LFM in the case of silica, a brittle mineral common in shales. We have shown that the kerogen and kerogen-silica interface exhibit a significant ductility. The ductility at the scale of the constituents of shale can significantly affect the ductility of the shale rock itself even with small fraction of ductile inclusions. We illustrate this potential effect by considering the example of the particle pull out phenomenon.

References

- [1] Leblond J-B. Mécanique de la rupture fragile et ductile. Hermès Science, 2003.
- [2] Sih G C et al. Int J Fracture 1965;1:189.
- [3] Brochard L et al. Fracture toughness from molecular simulation: Application to bulk silica, microporous carbons and their interface. In preparation.
- [4] van Duin A C T et al. J. Phys. Chem. A 2001;105:9396.
- [5] Chenoweth K et al. J. Am. Chem. Soc. 2005;127:7192.
- [6] Hantal G et al. Chemistry and molecular reconstruction of kerogen-silica interfaces. In preparation.
- [7] Lucas J et al. Scripta Metall Mater 1995;32:743.
- [8] Karihaloo B et al. JMPS 1996;44:1565.
- [9] Jain S K et al. Langmuir 2006;22:9942.
- [10] Bower A and Ortiz M. JMPS 1991;39:815.
- [11] He M-Y and Hutchinson J W. Int J Solids Struct 1989;25:1053.